

The Madeira Mode Water

GEROLD SIEDLER, ANNI KUHL AND WALTER ZENK

Institut für Meereskunde, Kiel University, 2300 Kiel, F. R. Germany

(Manuscript received 16 July 1986, in final form 10 March 1987)

ABSTRACT

Quasi-homogeneous layers in vertical profiles of temperature and salinity in the eastern North Atlantic near Madeira indicate the existence of a subtropical Mode Water in the Eastern Basin. Temperature sections show a maximum horizontal extent of at least 500 km. The frequency distribution analysis of homogeneous layers in a historical XBT dataset shows a Mode Water formation region near and to the north of Madeira. This Mode Water is found at increasing depths and displaced to the west and southwest during the course of the year after its formation by wintertime convection. It disappears almost completely, due to mixing, before the next winter. Volume estimates suggest that this Madeira Mode Water in the eastern Atlantic accounts for 15–20% of the total Central Water formation in the corresponding density range as obtained from tracer studies in the North Atlantic gyre.

1. Introduction

It has been known since the early work of Wüst (1935) and Iselin (1936, 1939) that the vertical temperature and salinity structure of the Atlantic resembles the horizontal structure in the isopycnal outcrop regions. Montgomery (1938) provided the basic concept of the dominating physical processes involved, with water mass formation by incorporation into the seasonal thermocline and advection and isopycnal mixing in the permanent thermocline. Some components of the Central Water in the interior are found to be nearly homogeneous and apparently formed by surface layer winter convection. Worthington (1959, 1976) studied one major example of this type of water, the "18° Water," in the Sargasso Sea. This water mass is found during the whole year in a region far exceeding the winter generation area in the western North Atlantic. Similar water types were found in other parts of the world ocean, and Masuzawa (1969) introduced the name "Subtropical Mode Water," indicating the significant volumetric mode in temperature–salinity diagrams. McCartney (1977) subsequently used the term Mode Water for a type of water that is formed at the surface and can be traced after isolation beneath the seasonal thermocline and which contributes substantial volumetric modes to the Central Water masses. The classical parameters for tracing the Central Water from its formation region have been temperature and salinity. More recently, anthropogenic tracers have also been used for this purpose, particularly tritium, ^3H , and freons (Sarmiento et al., 1982; Sarmiento, 1983; Jenkins, 1980, 1987; Thiele et al., 1986). In the absence of diapycnal mixing and for flow with small Rossby

number in the interior regime, potential vorticity is also an appropriate tracer for following Central Water masses across latitude circles. McCartney (1982) reviewed the available data on subtropical Mode Waters, particularly using potential vorticity for identification.

In the North Atlantic Ocean, only one formation region and one type of subtropical mode water was known, the 18° Water in the western North Atlantic. McCartney (1982) states, "In the eastern North Atlantic, there is no convective source for low potential vorticity of Eighteen Degree Water densities, and only isolated mesoscale cells of Eighteen Degree Water are found." We will demonstrate that, contrary to his conclusion, another formation area for subtropical mode water exists in the eastern North Atlantic Ocean. This water can be traced after isolation from the surface on its path from the formation region. In contrast to other types of mode water, however, the resulting homogeneous water mass contributes to the volumetric mode of the North Atlantic Central Water for only part of the annual cycle.

2. The data

In recent years studies such as the β -triangle surveys (Armi and Stommel, 1983) and the observations of the Kiel Warmwassersphäre Program (Stramma, 1984; Siedler et al., 1985) have added new information on the water mass distribution and the recirculation of the North Atlantic gyre in the Eastern Basin. Several cruises were conducted near Madeira where, on a number of occasions, quasi-homogeneous layers were noticed with temperatures near 18°C and below (Käse et al., 1985, 1986). Some examples are given of vertical profiles and

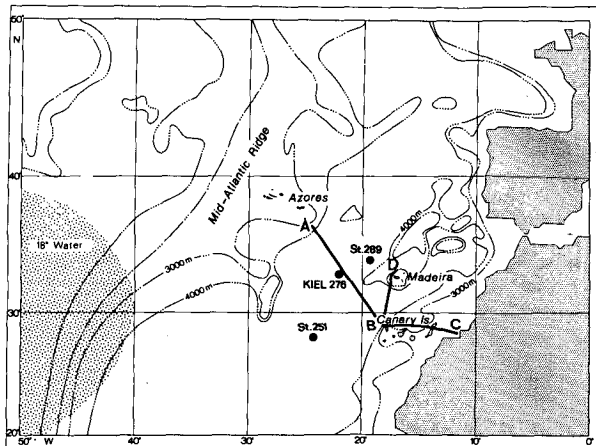


FIG. 1. Map of Madeira area with selected CTD stations (see Fig. 2), mooring KIEL 276 (see Fig. 3) and XBT sections (see Figs. 4, 5). Shaded area indicates approximate extent of Sargasso Sea 18° Water after Worthington (1976).

sections that were obtained in the Kiel Warmwassersphäre program. A map of the area is shown in Fig. 1.

Two CTD stations from the Canary Basin are presented in Fig. 2. The left-hand diagram shows the homogeneous surface layer in early April formed by convection in winter. The right-hand diagram shows an example from November, with the seasonal thermocline and mixed layer above and a layer of low temperature gradient with temperatures near 18°C in the depth range 100–200 m below. The properties of this quasi-homogeneous layer approximately correspond to those of the wintertime surface layer. A change in temperature from 18° to 16°C corresponds to a σ_t change of approximately 26.55 to 26.75 kg m^{-3} .

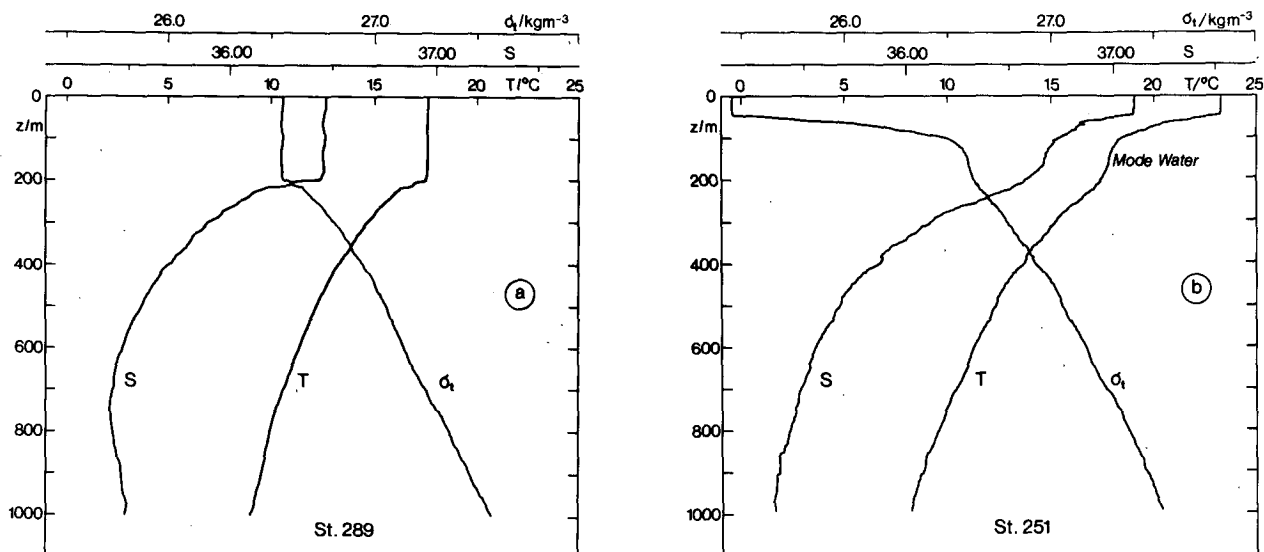


FIG. 2. Typical April (a) and November (b) vertical profiles of temperature T , salinity S and density σ_t in the Madeira area. (Station 289, 2 April 1982, 34°00'N, 19°36'W; station 251, 3 November 1984, 28°00'N, 24°31'W.)

An example of the temporal temperature change in the upper thermocline is given in Fig. 3 by a subset of 11 temperature time series from between 197 and 247 m depth, observed at the mooring KIEL 276 (33°12'N, 21°54'W) west of Madeira. In March, the temperatures at the upper sensors increase to approximately 18°C several times. A complicated history of downward-mixing of the surface layer in winter is apparent. Advection, however, will also be important. Internal waves were eliminated from these records by applying a low-pass filter with a 30 h cutoff period. In this case, the maximum depth of the convective layer is approximately 200 m.

The spatial distribution of the spring surface mixed layer formed by wintertime convection is illustrated in Fig. 4. In the area between the Azores and the West African coast, the well-mixed layer with a temperature of approximately 18°C is bounded by the Azores Front (Käse and Siedler, 1982) in the northwest and by coastal upwelling areas in the east. Two summer sections from the Azores (A) to the Canary Islands (B) and from there towards the Iberian Basin (D) are presented in Fig. 5. The relics of the wintertime surface mixed layer can be seen in the temperature range 16°–18°C where larger isotherm spacing (a , b) indicates low vertical gradients. The corresponding inverse of the gradient is presented in the lower sections, and maxima are found between 16° and 18°C (c , d). The horizontal extents are about 500 and 300 km. It is probable that the layers of maximum $\Delta z/\Delta T$ occurring just north and just northwest of position B were part of the same feature and extend from one section to the other (see inserted map).

If the inverse temperature gradient maxima identify mode water that was originally formed at the surface

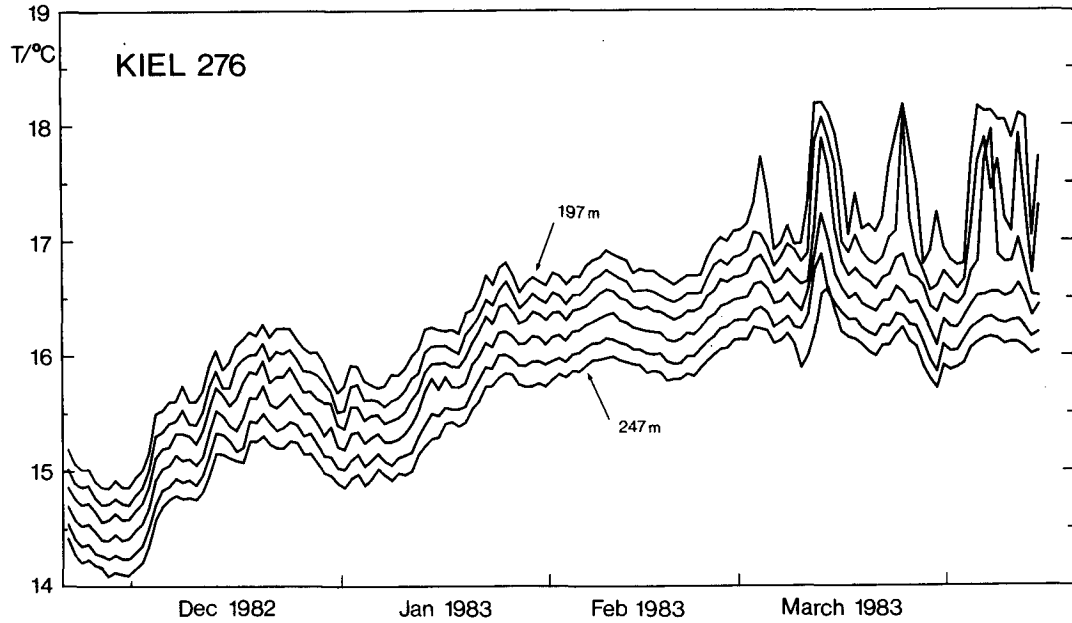


FIG. 3. Temperatures in the upper thermocline from mooring KIEL 276 west of Madeira (for position see Fig. 1), with the Mode Water formation process appearing in spring. The vertical separation of the sensors was 10 m.

in winter, the outcrop of the corresponding densities ($\sigma_t = 26.5$ to 26.8 kg m^{-3}) will indicate the wintertime formation region. Figure 6a shows the outcrops of selected isopycnals obtained by several authors using averaged data. Major differences exist near the West African coast and near the Mid-Atlantic Ridge north of the Azores. Individual cases from quasi-synoptic surveys in the Kiel Warmwassersphäre Program for σ_t

$= 26.5 \text{ kg m}^{-3}$ are presented in Fig. 6b and show considerable deviations from the averaged data. A shift is found towards the north in the area south of the Azores, and a more meridional orientation of the isopycnal outcrop near mooring KIEL 276. Judging by these case studies, a formation region for mode water with σ_t near 26.5 can be expected in the vicinity of this mooring, i.e., close to Madeira.

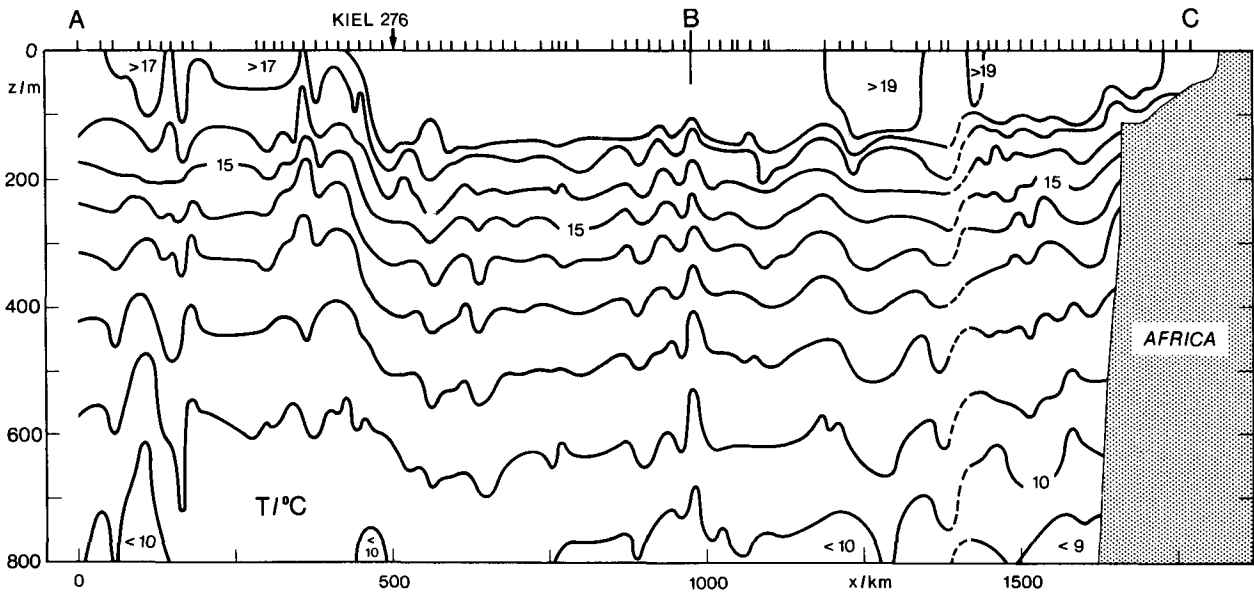


FIG. 4. Temperature section between the Azores (A), the Canary Islands (B) and the west coast of Africa (C) in March 1982. For position see Fig. 5. The Azores Front is seen on the left, an upwelling region on the right side. The surface mixed layer formed by winter convection can be seen between these two regions.

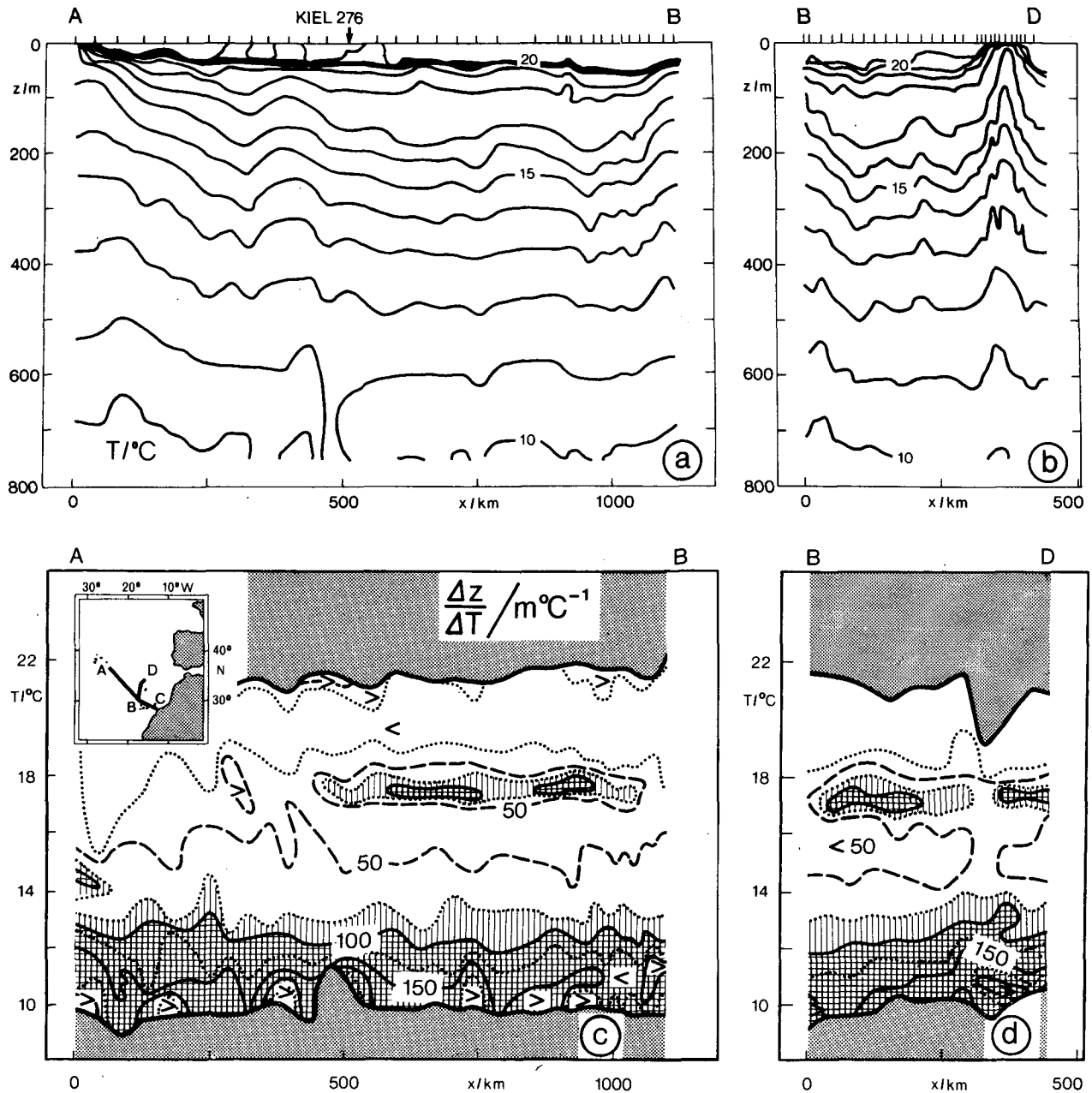


FIG. 5. Temperature sections A-B (a) and B-D (b) in July 1981 and corresponding sections (c, d) of $\Delta z/\Delta T$, with maxima between 16° - 18°C indicating the extent of the Mode Water.

After having obtained evidence for the existence of extensive volumes of water with mode water properties in the eastern North Atlantic, other temperature data from this region were reviewed. It was hoped to obtain the areal distribution of water mass formation, the path of mode water after being isolated from the surface, and the formation rate. A data source was provided by the international expendable bathythermograph (XBT) dataset. For the region 0° to 60°N , 0° to 50°W , a total of 27 519 XBT profiles were received from the U.S.

National Oceanographic Data Center, with characteristic points given with a nominal accuracy of $\pm 0.2^{\circ}\text{C}$ and ± 2 m. All profiles with data only in the upper 100 m were eliminated, thus excluding shallow-water and incomplete profiles, leaving a total of 27 441 profiles. The data were grouped into seasonal classes, centered on the later part of the seasons, winter (January-March), spring (April-June), summer (July-September) and fall (October-December), and were then grouped in $5^{\circ} \times 5^{\circ}$ squares. It was assumed that the

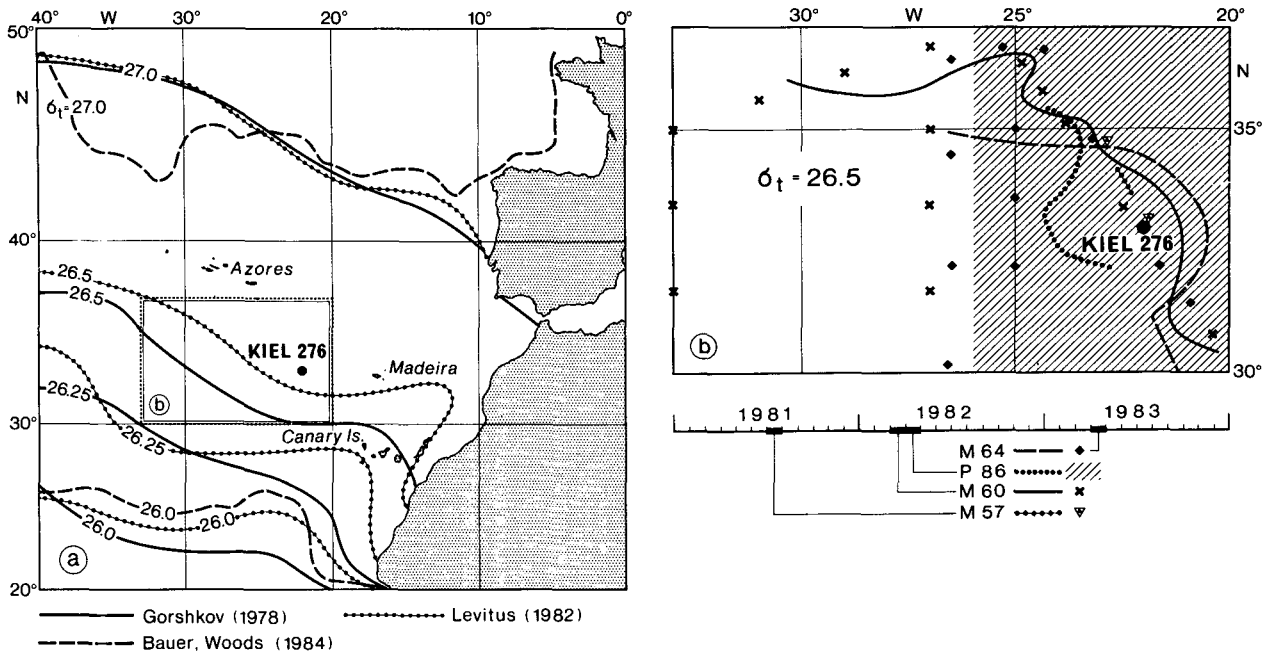


FIG. 6. Locations of density outcrop regions, determined by several authors from averaged data (a), and for particular cases of quasi-synoptic datasets obtained in the present study (b). *M* and *P* refer to *Meteor* and *Poseidon* cruise numbers, respectively.

spatial distribution of profiles within each square was sufficiently uniform in the area of main interest so as to preclude significant bias errors. The resulting distributions of the number of profiles per square and season are given in Fig. 7. A good data coverage can be seen in the area near Madeira which is of main interest here. In the later discussion of homogeneous layers, all squares with 20 or fewer profiles will be disregarded.

The data of temperature (*T*) vs depth (*z*) were fitted with cubic splines, smoothed using a running mean, and differentiated by determining $\Delta T/\Delta z$ with $\Delta z = 10$ m. To identify homogeneous water masses in the surface layer and the upper and the main thermocline, profiles of $\Delta T/\Delta z$ were grouped into three depth classes: 0–70 m, 70–160 m and 160–450 m. These three layers were selected in order to facilitate presenting the migration of surface-formed water towards greater depths,

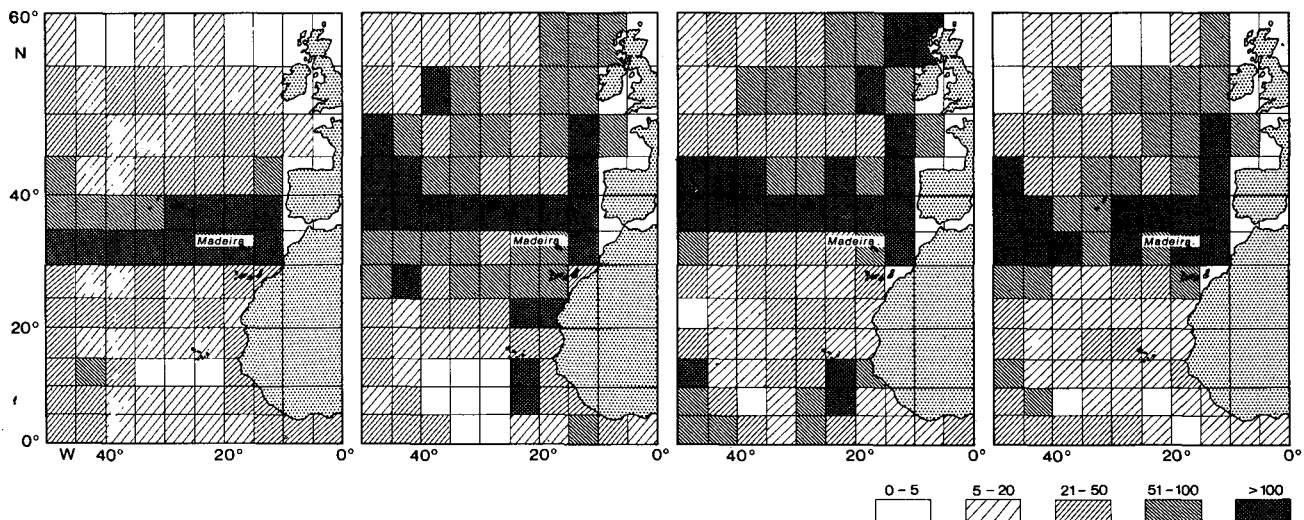


FIG. 7. Classes of XBT profile numbers per 5° × 5° square and season (winter–spring–summer–fall from left to right).

with the following rationales for determining the layer boundaries: the layer 0–70 m covers the range of the seasonal mixed layer in summer, the layer 70–160 m includes most of the isolated homogeneous water, and the lower limit of the third layer between 160 and 450 m is given by the maximum depth of the XBT profiles.

A criterion for homogeneity in temperature that took into account possible measurement errors and data smoothing effects had to be established. It was decided to use a threshold gradient of $0.007^{\circ}\text{C m}^{-1}$, and a minimum layer thickness of 50 m. This corresponds to a value of $0.35^{\circ}\text{C}/50\text{ m}$, a temperature difference well above the expected errors. Inspection of CTD data from the area suggested selecting two temperature ranges for the following analysis, 16° – 17°C and 17° – 18°C . Thermostads were identified in both of these two temperature ranges.

3. Spatial and seasonal variations of Mode Water occurrence

Homogeneous water as defined by the above conditions occurs only in a fraction of the profiles belonging to a certain $5^{\circ} \times 5^{\circ}$ square and season. The frequency of occurrence p_{jk} in square j and layer k for each season can be computed for each j , k and season. In order to exclude homogeneous layers that are exposed to the atmosphere, capped layers are identified by comparing the temperature at 10 m depth with the temperature 10 m below the upper limit of the homogeneous layer. If the 10 m depth value exceeds the other value by 0.5°C or more, the layer is considered a capped layer. By multiplying the frequency of capped layers with the mean thickness h_{jk} and surface area F_j a measure for the mean volume $v_{jk} = F_j h_{jk} p_{jk} = F_j D_{jk}$ is obtained. Examples illustrating the computational steps are presented in Fig. 8. The coasts of the Iberian Peninsula and Northwest Africa are approximated by the solid line, the Mid-Atlantic Ridge is indicated by the dotted line. In order to smooth the transition between the columns for the individual $5^{\circ} \times 5^{\circ}$ squares in the three-dimensional presentation, a 3×3 plotting grid was used for each $5^{\circ} \times 5^{\circ}$ square.

Two peaks are seen in the plots of Fig. 8, one near Madeira and a well-separated peak west of the Mid-Atlantic Ridge. The western peak compares well with the known distributions of the 18° Water formed in the Sargasso Sea (see Fig. 1). The eastern peak is related to another formation region. The winter convection area of this water mass can be seen in Fig. 9 where the layer thicknesses D in the upper 70 m are given for each $5^{\circ} \times 5^{\circ}$ square and for the four seasons. The formation and spreading area is approximately centered near Madeira. The subtropical mode water of the eastern North Atlantic is therefore named "Madeira Mode Water." The annual cycle of the production of homogeneous water in the surface layer in winter and its disappearance due to capping by the formation of

a surface mixed layer in spring and summer is clearly seen. The increasing values in fall (October–December) indicate the onset of convection due to cooling late in the year.

The history of homogeneous layers formed at the surface in winter with capping in spring is summarized in the set of diagrams in Fig. 10 for the temperature range 17° – 18°C . Since only capped layers are presented here, low values are found in the 0–70 m layer throughout the year, with the exception of the Sargasso Sea water portion in spring. The relics from the wintertime surface layer cause increased values in the 70–160 m depth range in spring and summer, and increased values in the 160–450 m depth range in summer. The path of spreading of the water formed in winter can be obtained from the displacement of the maxima in the region east of the Mid-Atlantic Ridge. See for example the sequence of peaks in the following diagrams:

- 1) Winter: 0–70 m (Fig. 9)
- 2) Spring: 0–70 m (Fig. 10)
- 3) Summer: 70–160 m (Fig. 10)
- 4) Fall: 160–450 m (Fig. 10).

From these we conclude that the Madeira Mode Water in the 17° – 18°C range is formed close to Madeira and is transported towards the west and somewhat to the south during the course of the year. While the western North Atlantic Subtropical Mode Water is found during all four seasons, its eastern counterpart disappears almost completely due to mixing processes within the interval of a few months.

Similar distributions are found for the 16° – 17°C range (not presented here). There is a distinctive difference, however, in the shape of the eastern Mode Water distribution. While the 17° – 18°C Mode Water is centered rather tightly around Madeira or further to the west later in the year, the 16° – 17°C Mode Water is found about 5° further to the north, with a zonally banded structure.

4. The annual rate of Mode Water formation

The eastern Mode Water is sufficiently well defined in space to attempt the determination of its total volume for each season. There remains some arbitrariness, however, in separating the western and the eastern Mode Water. The distributions suggest a separation line near the Mid-Atlantic Ridge at 35°W , and this line is used for the volume analysis. In addition, zonal boundaries between 20° and 35°N were used for the 17° – 18°C range (see Fig. 8b), and 20° and 40°N for the 16° – 17° range. The resulting volumes of Madeira Mode Water are presented in Table 1 and Fig. 11.

The errors given in Table 1 were determined in the following way (all volumes refer to the areas between the above boundaries), with the symbols:

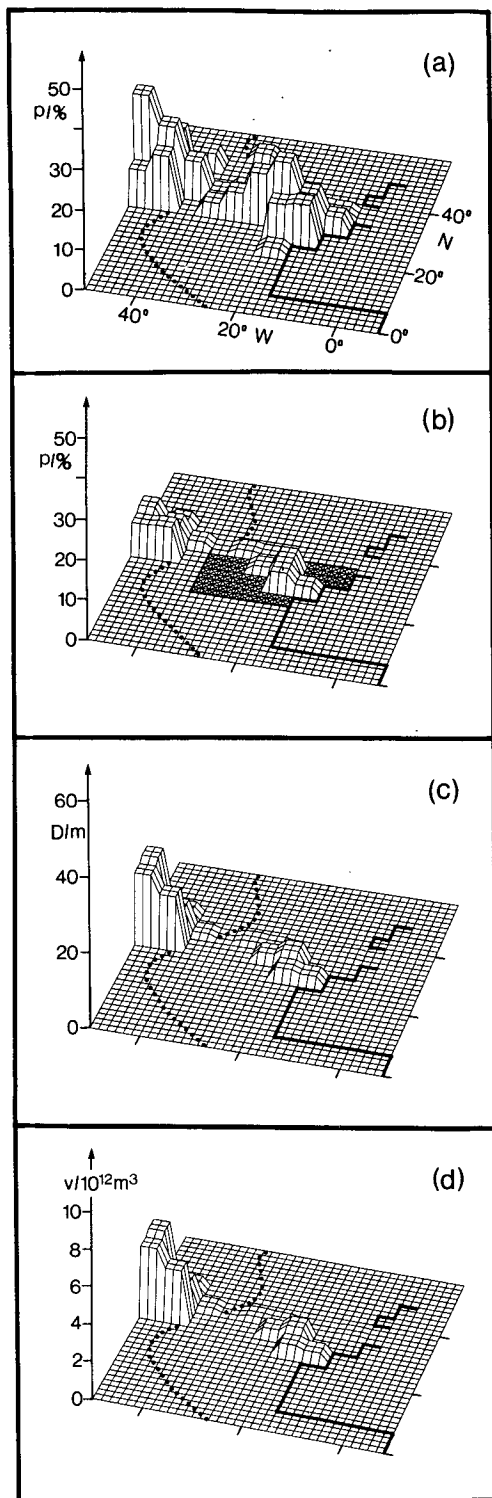


FIG. 8. Examples illustrating the steps of determining the location, frequency and volume of homogeneous layers, for the case 17°–18°C, 0–70 m, spring: Frequency of profiles with homogeneous layers per 5° × 5° square (a), frequency of profiles with capped layers (b), layer thickness *D* given by frequency of profiles with capped layers multiplied by mean layer thickness *h* (c), and volume *v* given by frequency of capped layers multiplied by mean layer thickness and

- k* number of layer from above (1, 2, 3)
- m* total number of 5° × 5° squares
- j* number of square
- N_j* total number of profiles, square *j*
- n_{jk}* number of profiles with capped layers, square *j*, layer *k*
- h_{jk}* mean thickness of capped layers, square *j*, layer *k*
- p_{jk}* *n_{jk}/N_j* = frequency of capped layers, square *j*, layer *k*
- F_j* surface area, square *j*.

The total volume of capped mode water layers in square *j* and layer *k* is then given by

$$v_{jk} = F_j h_{jk} p_{jk}.$$

The total volume in layer *k* for all squares is given by

$$v_k = \sum_{j=1}^m v_{jk}.$$

The total Madeira Mode Water volume results from

$$v = \sum_{k=1}^3 v_k.$$

The rms error Δv_{jk} of v_{jk} is obtained from

$$\Delta v_{jk} = \left[\left(\frac{\partial v_{jk}}{\partial F_j} \right)^2 \Delta F_j^2 + \left(\frac{\partial v_{jk}}{\partial h_{jk}} \right)^2 \Delta h_{jk}^2 + \left(\frac{\partial v_{jk}}{\partial p_{jk}} \right)^2 \Delta p_{jk}^2 \right]^{1/2}.$$

The computational error ΔF_j is negligible. The mean thickness error Δh_{jk} is assumed to be ±10 m; the relative error of p_{jk} is assumed to be 10%, or $0.1 p_{jk}$. One obtains

$$\Delta v_{jk} = [(F_j p_{jk} \times 10)^2 + (F_j h_{jk} \times 0.1 p_{jk})^2]^{1/2}.$$

The rms errors of v_k and v are given by

$$\Delta v_k = \left[\sum_{j=1}^m (\Delta v_{jk})^2 / (m - 1) \right]^{1/2} \quad \Delta v = \left(\sum_{k=1}^3 \Delta v_k^2 / 2 \right)^{1/2}.$$

These absolute errors are presented in Table 1, and the relative errors in percent are also given for the total volumes per temperature range and season. The observed changes of mode water volumes are well above the error limits, and this would still be true with more pessimistic assumptions for Δh_{jk} and Δp_{jk} .

The fact that the Madeira Mode Water does not persist during the whole year makes it possible to estimate the mean annual rate of formation, or rather the lower limit of this rate given by the maximum total volume of capped homogeneous layers in one season. As expected, we find the maximum in spring, both for 17°–18°C and 16°–17°C. The rate of Madeira Mode Water formation is then obtained from Table 1, namely

surface area (d). The shaded area in (b) indicates the integration area selected for determining the volume of 17°–18°C Madeira Mode Water.

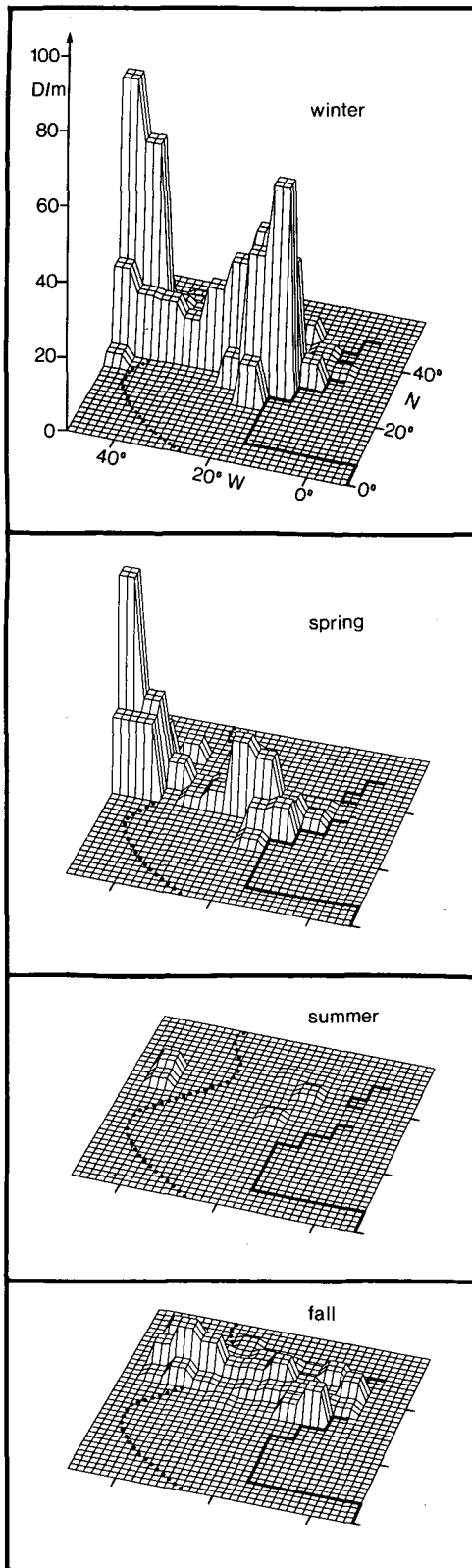


FIG. 9. Layer thickness D given by frequency of profiles with homogeneous layers multiplied by mean layer thickness h , for the case: 17° – 18° C, 0–70 m, four seasons.

17° – 18° C:

$$17.2 \times 10^{12} \text{ m}^3 \text{ yr}^{-1} = 0.55 \times 10^6 \text{ m}^3 \text{ s}^{-1} \equiv 0.55 \text{ Sv}$$

16° – 17° C:

$$22.7 \times 10^{12} \text{ m}^3 \text{ yr}^{-1} = 0.72 \times 10^6 \text{ m}^3 \text{ s}^{-1} \equiv 0.72 \text{ Sv}.$$

The Madeira Mode Water is part of the total volume of ventilated thermocline water in the subtropical gyre. The formation rate will therefore be smaller than the rate obtained from total Central Water renewal estimates. Sarmiento (1983) determined exchange rates from a tritium box model of the North Atlantic thermocline and from Ekman pumping. He obtained numbers between 3.4 and 4.1 Sv and between 0.66 and 0.73 Sv, respectively, for layers with $\Delta\sigma_{\theta} = 0.1 \text{ kg m}^{-3}$ in the range corresponding to the 16° – 18° C water. The mode water formation rates found here are lower than the tritium box model results by a factor of 5 to 7. Considering the horizontal and vertical extent of the Madeira Mode Water compared with the total ventilated North Atlantic thermocline water, the formation rate appears reasonable. It should be kept in mind, however, that our numbers for the Madeira Mode Water represent lower limits of mean rates. The actual formation rates can be larger and will probably vary from year to year.

5. Discussion

Evidence has been presented for the existence of subtropical mode water in the eastern North Atlantic, with maximum horizontal extents of at least 500 km, i.e., larger than that of isolated mesoscale cells. The statistical approach to the analysis of XBT data leads to the following main results. The formation region is centered near Madeira for Mode Water in the 17° – 18° C range, bounded by the Azores Front to the northwest. The formation region for the 16° – 17° C range lies further to the north. After capping of the winter surface layer during the formation of the seasonal thermocline, the mode water is found at increasingly greater depths during the course of the year, with the maxima in volume distributions shifting to the west and southwest from spring to summer. From distributions of the baroclinic flow field in this area (Stramma, 1984) a stronger southward component of the mode water advection might be expected. The early stages of this advection near the surface will, however, be strongly controlled by the Ekman transport which is to the west in the region under consideration (Stramma and Isemer, 1986). A movement of the distribution peaks by one or two $5^{\circ} \times 5^{\circ}$ squares is not inconsistent with velocities expected. A source region for Central Water near Madeira could have been guessed from Sarmiento's (1983) maps of the tritium distribution at $\sigma_{\theta} = 26.5$ and 26.8 .

Why was the subtropical mode water of the eastern North Atlantic not found in the earlier studies? There are several reasons. The Madeira Mode Water is re-

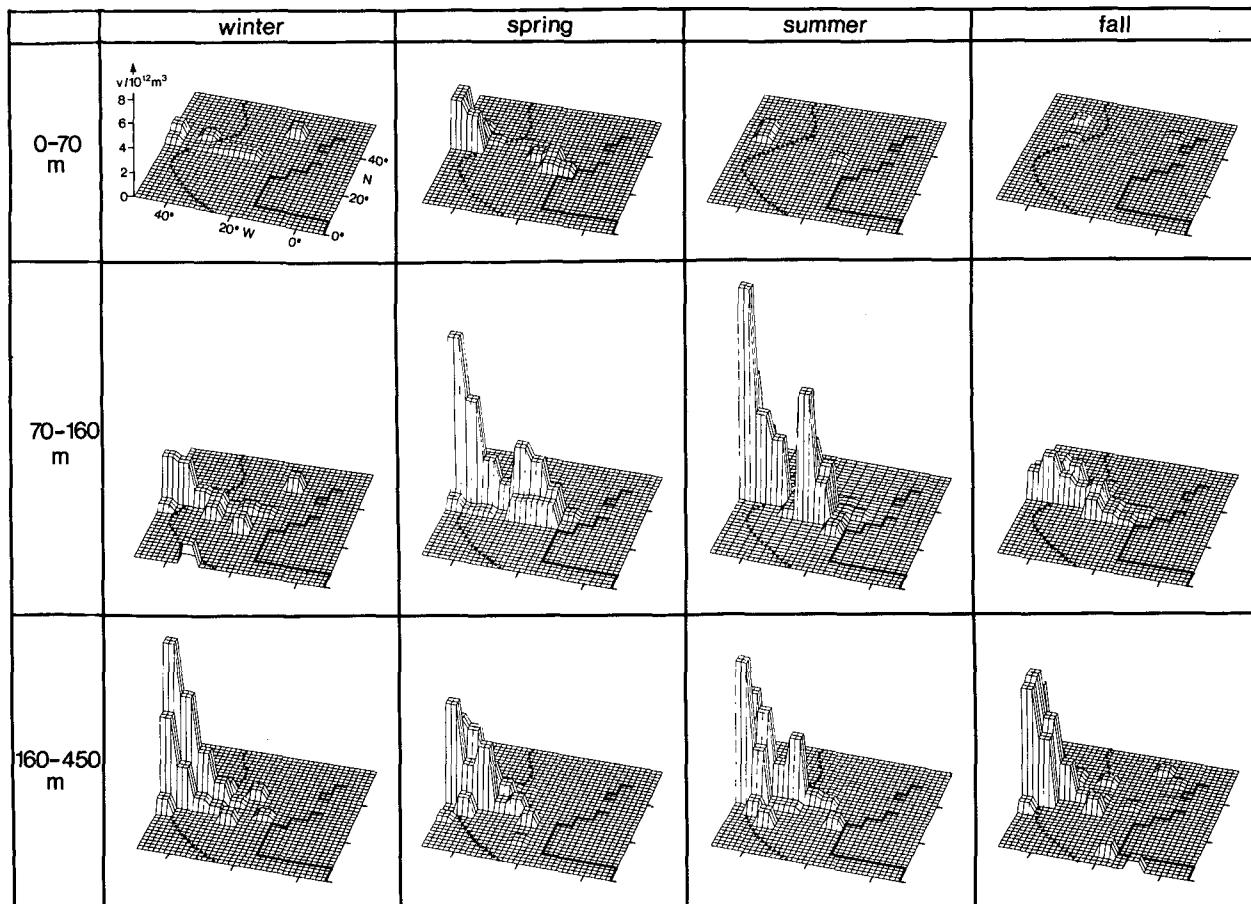


FIG. 10. Volume v of capped layers for the case 17° – 18° C, three depth ranges, four seasons.

stricted in horizontal extent and disappears almost completely due to mixing after about six months and, furthermore, the relevant section in the Eastern Basin

analyzed by McCartney (1982) was located at 36° N, just north of the formation region determined in the present study.

TABLE 1. Volume of Madeira Mode Water.

Depth range (m)	Volume (10^{12} m ³) for the seasons			
	Jan-Mar	Apr-Jun	Jul-Sep	Oct-Dec
17° – 18° C				
0–70	0.47 ± 0.09	3.24 ± 0.15	0.31 ± 0.06	0.12 ± 0.03
70–160	2.40 ± 0.21	12.72 ± 0.55	11.06 ± 0.43	2.16 ± 0.10
160–450	0.51 ± 0.11	1.19 ± 0.24	1.70 ± 0.23	0.19 ± 0.03
0–450	3.4 ± 0.2 ($\pm 5.3\%$)	17.2 ± 0.4 ($\pm 2.6\%$)	13.1 ± 0.3 ($\pm 2.6\%$)	2.5 ± 0.1 ($\pm 3.0\%$)
16° – 17° C				
0–70	0.33 ± 0.04	3.75 ± 0.11	0.20 ± 0.01	0.69 ± 0.03
70–160	4.61 ± 0.18	15.15 ± 0.31	8.07 ± 0.27	4.44 ± 0.14
160–450	2.07 ± 0.08	3.78 ± 0.10	8.53 ± 0.28	4.50 ± 0.13
0–450	7.0 ± 0.1 ($\pm 2.1\%$)	22.7 ± 0.2 ($\pm 1.1\%$)	16.8 ± 0.3 ($\pm 1.6\%$)	9.6 ± 0.1 ($\pm 1.4\%$)

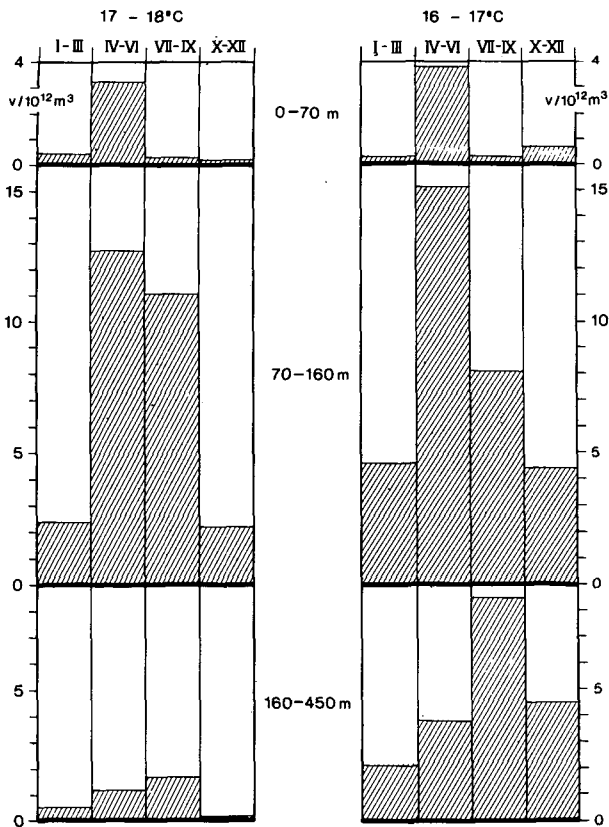


FIG. 11. Seasonal change of capped layer volume v east of 35°W in three depth ranges for each season for the temperature ranges 17° – 18°C and 16° – 17°C .

The Madeira Mode Water provides a useful tracer for Central Water ventilation studies due to its temporal and spatial distribution limits. It provides 15% to 20% of the volume of ventilated thermocline water in the respective density range in the North Atlantic. Small subvolumes may be preserved within isolated core water over extended periods in mesoscale eddies while being advected over large distances in the subtropical gyre. McDowell (1986) recently demonstrated that anomalous salinity–oxygen features on the potential density surface $\sigma_\theta = 26.507 \text{ kg m}^{-3}$ found in the Sargasso Sea can be related to a source region near 33°N , 30°W , i.e., in the western part of the Madeira Mode Water region.

Acknowledgments. The authors thank M. Zwierz, B. Klein and R. Budich for their assistance in data processing. We have also benefited from discussions with H. Leach. The study was funded by the Deutsche Forschungsgemeinschaft (DFG, SFB 133).

REFERENCES

- Armi, L., and H. Stommel, 1983: Four views of a portion of the North Atlantic subtropical gyre. *J. Phys. Oceanogr.*, **13**, 828–857.
- Bauer, J., and J. D. Woods, 1984: Isopycnic Atlas of the North Atlantic Ocean. *Ber. Inst. f. Meeresk. Kiel*, **132**, 173 pp.
- Gorshkov, S. G., 1978: *World Ocean Atlas*, 2. Pergamon Press, 306 pp.
- Iselin, C. O'D., 1936: A study of the circulation of the western North Atlantic. *Pap. Phys. Oceanogr. Meteor.*, **4**(4), 101 pp.
- , 1939: The influence of vertical and lateral turbulence on the characteristics of water at middepths. *Trans. Amer. Geophys. Union*, **20**, 414–417.
- Jenkins, W. J., 1980: Tritium and ^3He in the Sargasso Sea. *J. Mar. Res.*, **38**, 533–569.
- , 1987: ^3H and ^3He in the beta triangle: Observations of gyre ventilation and oxygen utilization rates. *J. Phys. Oceanogr.*, **17**, 763–783.
- Käse, R. H., and G. Siedler, 1982: Meandering of the subtropical front southeast of the Azores. *Nature*, **300**(5889), 245–246.
- , W. Zenk, T. B. Sanford and W. Hiller, 1985: Currents, fronts and eddy fluxes in the Canary Basin. *Progress in Oceanography*, Vol. 14, Pergamon, 231–257.
- , J. F. Price, P. L. Richardson and W. Zenk, 1986: A quasi-synoptic survey of the thermocline circulation and water mass distribution within the Canary Basin. *J. Geophys. Res.*, **91**(C8), 9739–9748.
- Levitus, S., 1982: *Climatological Atlas of the World Ocean*. NOAA, Rockville, MD, Prof. Paper 13, 173 pp.
- Masuzawa, J., 1969: Subtropical Mode Water. *Deep-Sea Res.*, **16**, 463–472.
- McCartney, M. S., 1977: Subantarctic Mode Water. A Voyage to Discovery, supplement to *Deep-Sea Res.*, M. Angel, Ed., 103–119.
- , 1982: The subtropical recirculation of Mode Waters. *J. Mar. Res.*, **40**(Suppl), 427–464.
- McDowell, S. E., 1986: On the origin of eddies discovered during the POLYMODE Local Dynamics Experiment. *J. Phys. Oceanogr.*, **16**, 632–652.
- Montgomery, R. B., 1938: Circulation in upper layers of southern North Atlantic deduced with use of isentropic analysis. *Pap. Phys. Oceanogr. Meteor.*, **6**, No. 3, 55 pp.
- Sarmiento, J. L., 1983: A tritium box model of the North Atlantic thermocline. *J. Phys. Oceanogr.*, **13**, 1269–1274.
- , C. G. Rooth and W. Roether, 1982: The North Atlantic tritium distribution in 1972. *J. Geophys. Res.*, **87**, 8047–8056.
- Siedler, G., W. Zenk and W. J. Emery, 1985: Strong current events related to a subtropical front in the Northeast Atlantic. *J. Phys. Oceanogr.*, **15**, 885–897.
- Stramma, L., 1984: Geostrophic transports in the warm water sphere of the eastern subtropical North Atlantic. *J. Mar. Res.*, **42**, 537–558.
- , and H. J. Isemer, 1986: Meridional temperature fluxes in the subtropical eastern North Atlantic. *Deep-Sea Res.*, **33**, 209–223.
- Thiele, G., W. Roether, P. Schlosser, R. Kuntz, G. Siedler and L. Stramma, 1986: Baroclinic flow and transient tracer fields in the Canary–Cape Verde Basin. *J. Phys. Oceanogr.*, **16**, 814–826.
- Worthington, L. V., 1959: The 18° Water in the Sargasso Sea. *Deep-Sea Res.*, **5**, 297–305.
- , 1976: On the North Atlantic circulation. *Johns Hopkins Oceanographic Studies*, Vol. VI. Johns Hopkins University Press, 110 pp.
- Wüst, G., 1935: Schichtung und Zirkulation des Atlantischen Ozeans. *Die Stratosphäre. Wiss. Ergebn. Dt. Atl. Exped. "Meteor" 1925–1927*, Vol. 6, Part 1, No. 2, 180 pp.